Supplement al Figure S1

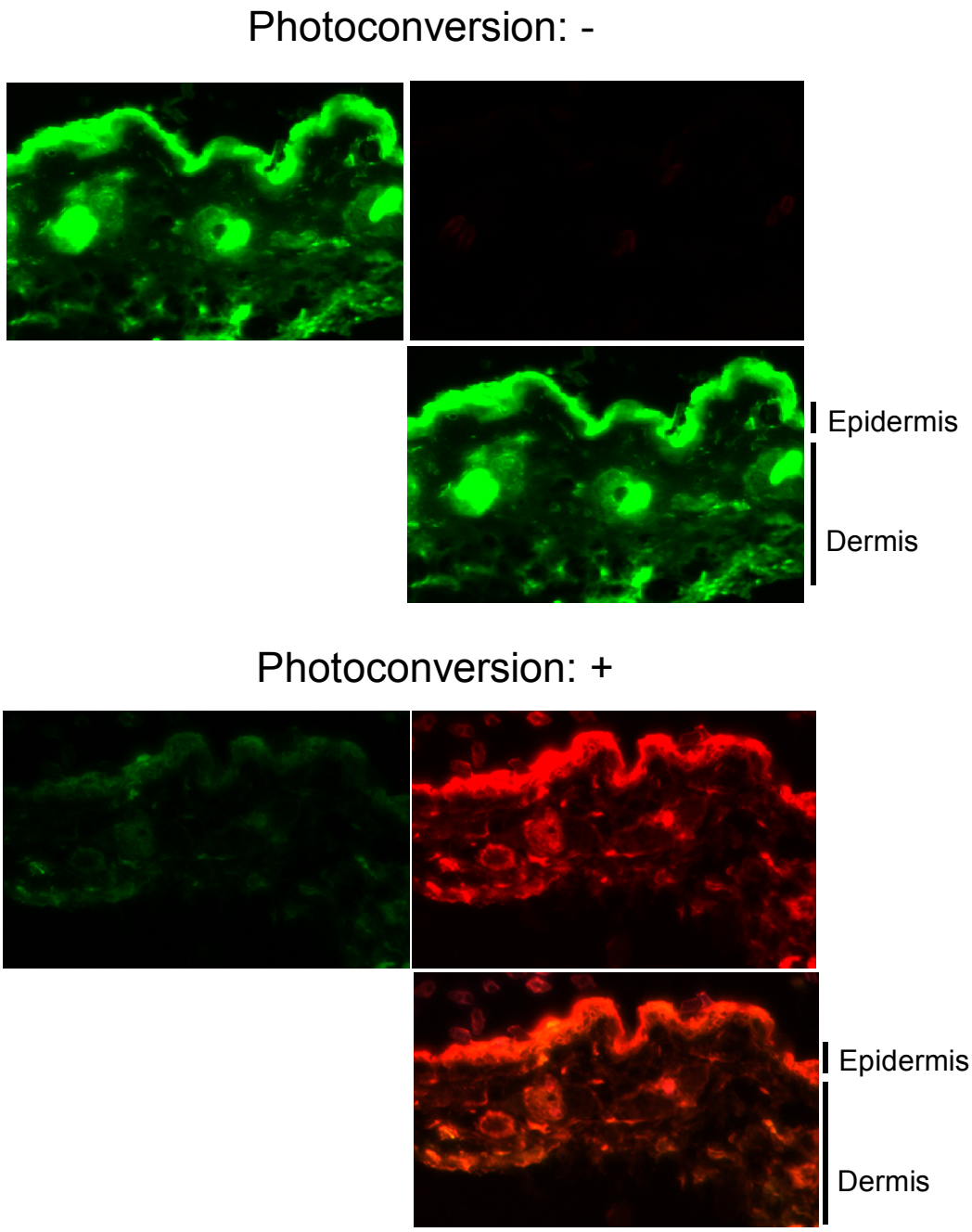

Supplemental Figure S2

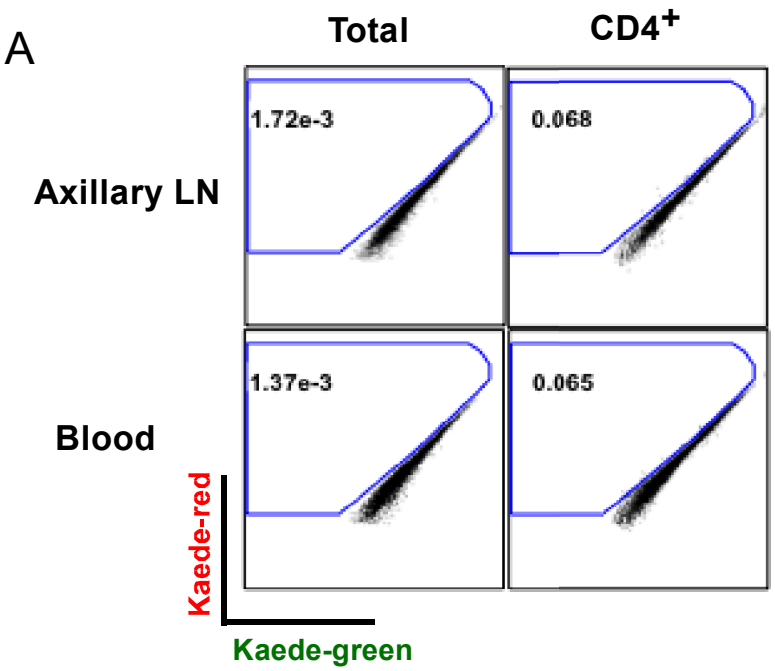

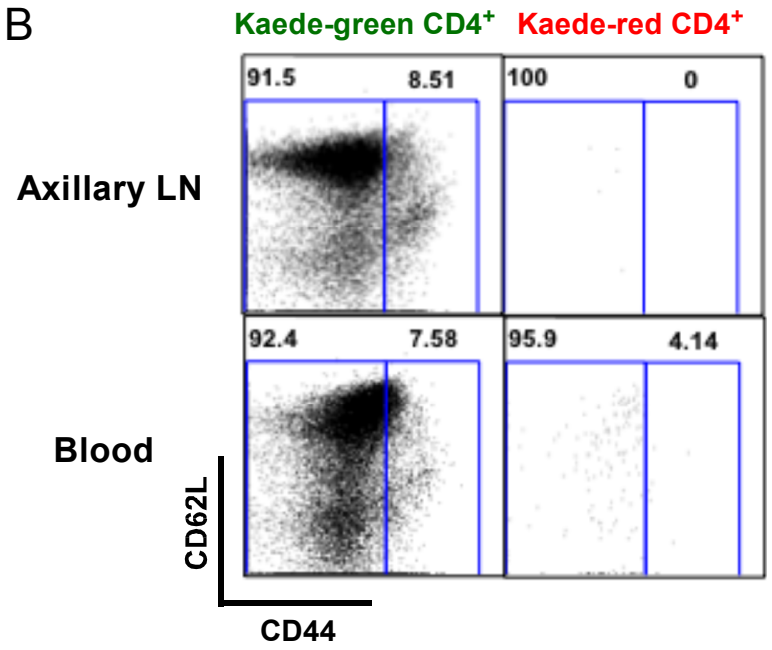

Supplemental Figure S3

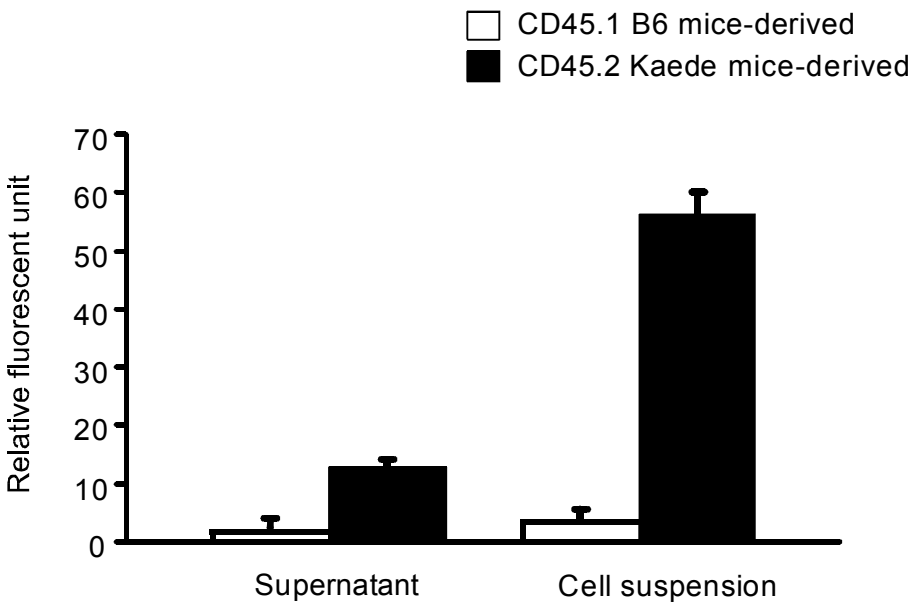

Supplemental Figure S4

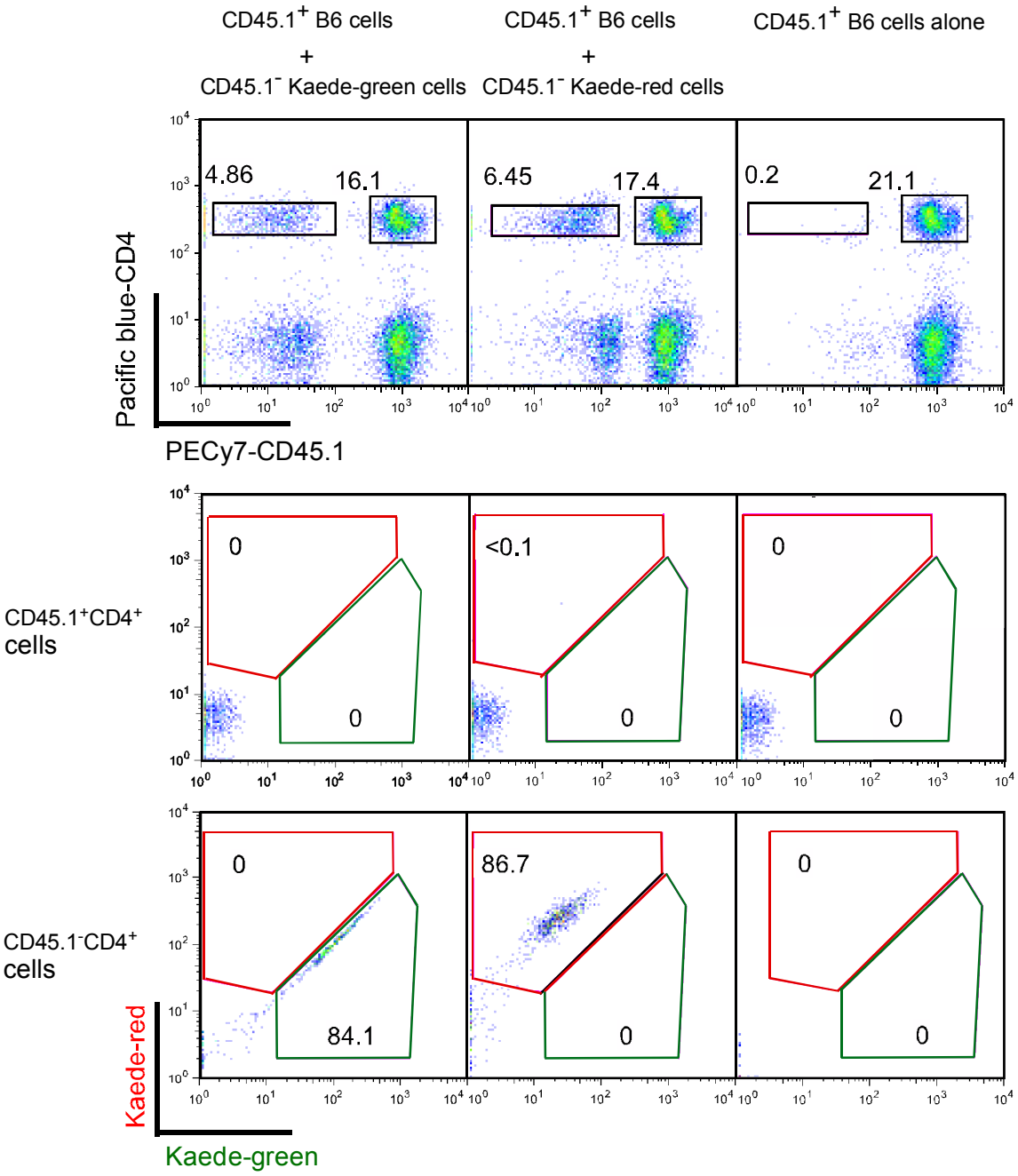

Supplemental Figure S5

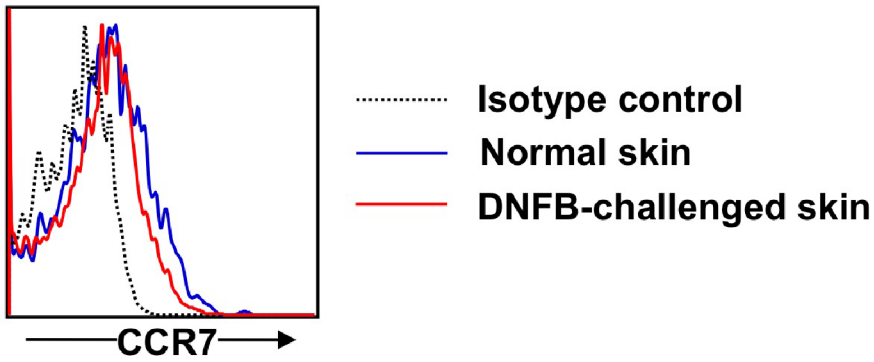

Supplemental Figure S6

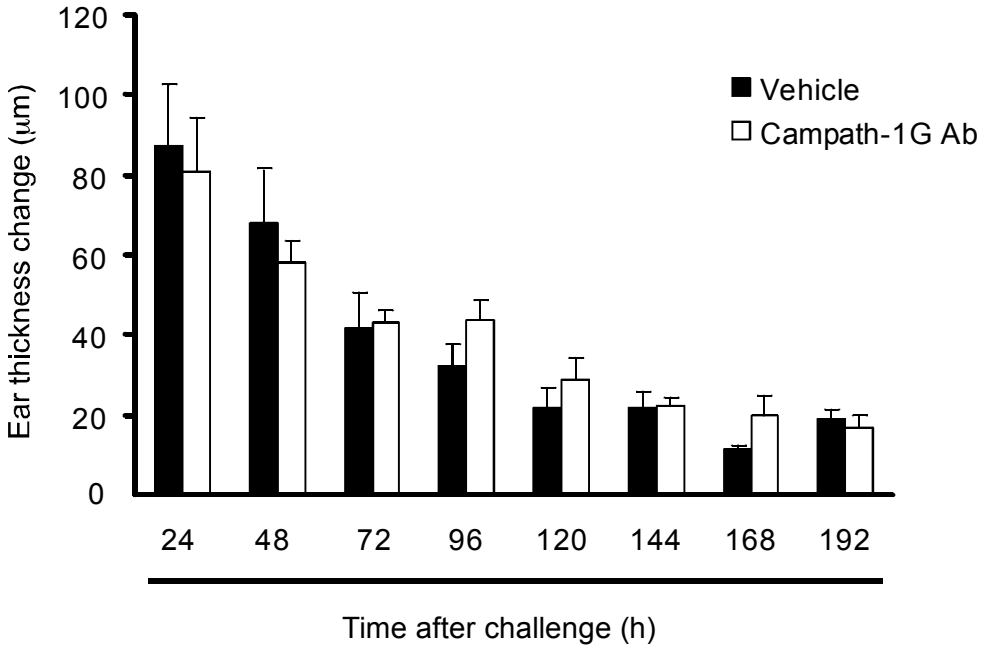

Supplemental Figure S7

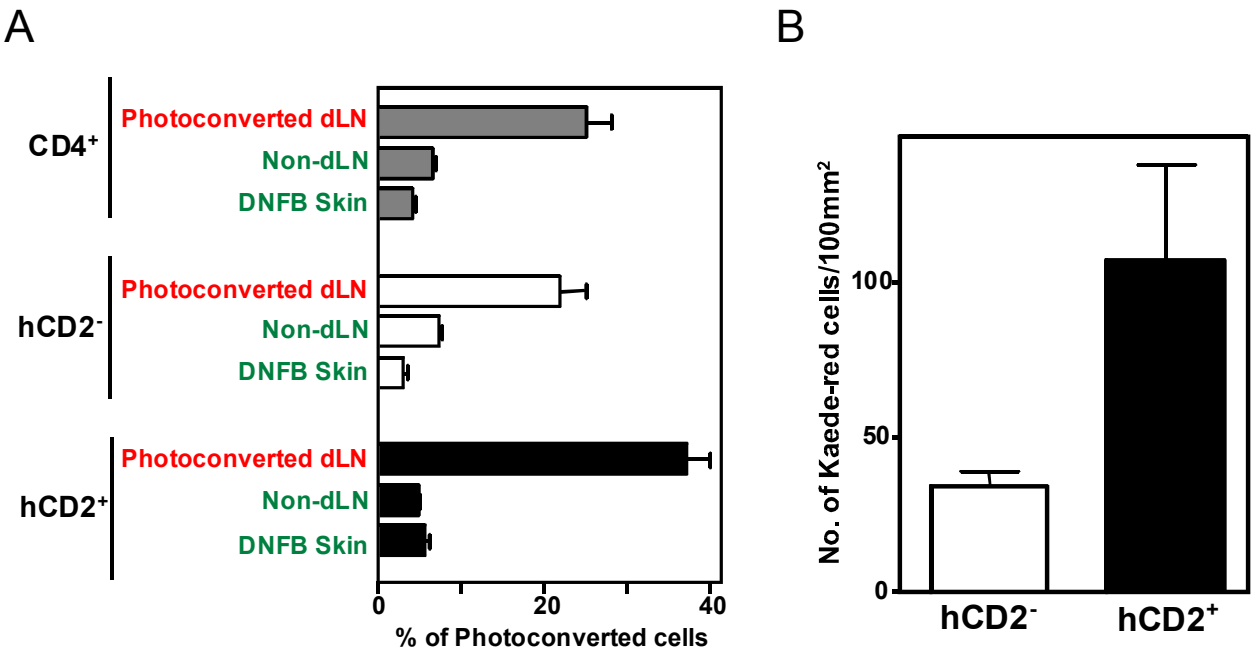

Supplemental Figure S8

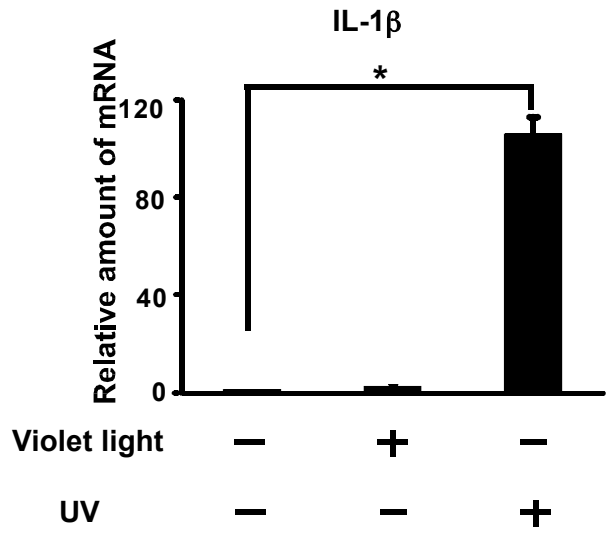

SUPPLEMENTAL FIGURE LEGENDS.

Supplemental Figure S1. Penetration of photoconversion in the skin.

The abdominal skin of Kaede/Foxp3$^{hCD2/hCD52}$ mice was photoconverted as described in Methods. After photoconversion, the skin was excised and fixed with 4% paraformaldehyde for 30 minutes, and then embedded in Tissue-Tek OCT compound. Frozen sections of skin tissues (10 μm) were observed with BioRevo (Keyence). Non-photoconverted skin (photoconversion:-) was used as a control for photoconverted skin (photoconversion:+). Images of green (upper left), red (upper right), and merged green and red (lower right) channels are shown.

Supplemental Figure S2. CD4$^+$T cell subsets in axillary lymph nodes and blood immediately after photoconversion of the skin.

(A) Immediately after photoconversion of the skin, marginal draining axillary LN cells and blood cells were collected, and total cells and CD4$^+$ cells were analyzed with flow cytometry to examine Kaede-red or Kaede-green. (B) Kaede-red and Kaede-green CD4$^+$ cells of axillary LNs and blood were further analyzed for the expression of CD44 and CD62L.

Supplemental Figure S3. Detection of Kaede-red proteins in the extracellular fluids.

Inguinal and axillary lymph nodes (3 x 10^6 cells) were taken from wild-type CD45.1$^+$ CD45.2$^-$ C57BL/6 mice and CD45.1$^-$ CD45.2$^+$ Kaede/Foxp3$^{hCD2/hCD52}$ mice, and the single cell suspensions were prepared in 1 ml of PBS. The cells were then exposed to

violet light (436 nm) for 10 min and incubated for 24 hours at 37°C. After incubation, the cell suspensions were centrifuged, and the supernatants were collected. The cell pellets were resuspended in 1 ml of PBS. Fluorescence of supernatant and cell suspension from wild-type CD45.1^{+} CD45.2^{-} C57BL/6 mice (CD45.1^{+} B6 mice-derived) and CD45.1^{-} CD45.2^{+} Kaede/Foxp3$^{hCD2/hCD52}$ mice (CD45.1^{-} Kaede mice-derived) was measured at an excitation wavelength of 561 nm and an emission wavelength of 600 nm with FlexStation (Bio-Rad laboratories).

Supplemental Figure S4. No incorporation of Kaede-red proteins by lymph node cells externally.

Inguinal and axillary lymph node cells were prepared from wild-type C57BL/6 (CD45.1^{+}) mice and Kaede/Foxp3$^{hCD2/hCD52}$ (CD45.1^{-}) mice as performed in Supplemental Figure S2. Subsequently, 3 x 10^5 LN cells from CD45.1 C57BL/6 mice were incubated either with or without LN cells from CD45.2 Kaede/Foxp3$^{hCD2/hCD52}$ mice that had been either photoconverted or non-photoconverted. After incubation for 24 hours, the cells were collected and expression of Kaede green and Kaede red signals in CD45.1^{+} and CD45.1^{-} CD4^{+} cells were examined by flow cytometry. The numbers in the figure indicate the frequency of the population (%).

Supplemental Figure S5. CCR7 expression of Tregs in the skin.

Ear cell suspensions were prepared from either the mice in the steady states or the mice 2 days after challenge of CHS response, and the expression level of CCR7 on hCD2 positive Tregs in the skin was determined by flow cytometry.

Supplemental Figure S6. No effect of Campath-1 treatment on CHS in B6 mice.

Time course of ear swelling response in CHS: The B6 mice were sensitized, and injected with vehicle or Campath-1G Ab before challenge. Ear thickness was measured every 24 h and the columns indicate average + SD (n=5 for each group).

Supplemental Figure S7. Migration of photoconverted $CD4^+$ T cells from draining lymph node to both non-draining lymph nodes and the skin.

(A, B) Kaede/$Foxp3^{hCD2/hCD52}$ mice were sensitized, challenged as in Figure 3A. Two days after challenge, bilateral draining axillary LNs were photoconverted and 24 h after photoconversion, the ears were re-challenged with 20 μl of 0.3% DNFB. Twenty-four hours after re-challenge, photoconverted Kaede-red $hCD2^-$ non-Tregs and $hCD2^+$ Tregs in photoconverted axillary LN, non-draining superficial cervical LNs, and the challenged ears were examined by flow cytometry. Percentages of photoconverted cells in each sample are indicated as mean + SD (n=3). In addition, the numbers of Kaede-red $hCD2^-$ non-Tregs and $hCD2^+$ Tregs in the challenged ears were measured (B). The numbers indicate mean + SD (n=3).

Supplemental Figure S8. IL-1β expression in the skin after photoconversion.

The abdominal skin of Kaede/$Foxp3^{hCD2/hCD52}$ mice was irradiated with violet light from Spot UV curing equipment (SP250; Ushio) or with UVB from Sunlamps emitting 280–360 nm with a peak emission at 312.5nm (FL 20SE, Toshiba Electric Co.). The skin of irradiated area was removed 6 hours after irradiation, and mRNA was extracted using TRIZOL. Then, mRNA expression of IL-1β were examined by quantitative

RT-PCR. The relative amounts of each gene are indicated as average + SD (n=3).